THE UNIVERSITY of EDINBURGH

Edinburgh Research Explorer

Optical phase and the ionization-dissociation dynamics of excited H-2

OPEN ACCESS

Optical phase and the ionization-dissociation dynamics of excited H2

A. Kirrander, H. H. Fielding, and Ch. Jungen

Additional information on J. Chem. Phys.

Optical phase and the ionization-dissociation dynamics of excited H₂

A. Kirrander,[1,a)] H. H. Fielding,[1,b)] and Ch. Jungen[2,c),d)]

[1]*Department of Chemistry, University College London, 20 Gordon Street, London WC1H 0AJ, United Kingdom*

[2]*Laboratoire Aimé Cotton du CNRS, Université de Paris-Sud, 91405 Orsay, France*

We investigate the influence of optical phase on the dynamics of hydrogen molecules excited to a spectral region with competition between predominantly rotational ionization, and dissociation. We show that an appropriate choice of optical phase changes the relative timing of the ionization and dissociation. Furthermore, the temporal width of the ionization and dissociation fluxes can also be controlled, in a matter-wave analogy of transform-limited optical pulses. The close link between the optical phase and the photoinduced electronic and molecular dynamics has important implications for femtochemistry. © *2010 American Institute of Physics.* [doi:10.1063/1.3285710]

I. INTRODUCTION

Shaping optical pulses[1] has become one of the key technologies in controlling the dynamics of molecules.[2–4] The complicated temporal evolution of quantum systems is extremely sensitive to phase, something which is illustrated dramatically in wave packet interferometry by multiple coherent optical pulses,[5–11] where the interference between subsequent pulses modulates the spectral amplitude and hence final product yields. Shaping the phase of a single optical pulse,[12] but leaving its spectral amplitude intact, offers a direct probe of the effect of optical phase on dynamics. The simplest example of a shaped phase is a linear chirp. A chirped pulse can be used to compensate partially for the anharmonicity in the vibrational states of diatomic molecules, allowing the wave packet to focus at certain internuclear distances.[13,14] Similarly, in the nonresonant continuum of simple atoms, linear chirp can be used to spatially focus ionized electron wave packets.[15,16] More complicated systems require more general phase shaping. In a recent paper we used phase-shaped pulses to localize a bound wave packet in a particular channel at a particular time in a two-channel model of rotationally and electronically excited H₂ molecules,[17] extending previous efforts to shape wave packets in simple atomic Rydberg systems.[18–21]

In this paper, a more intricate scenario is investigated by examining a realistic case of ionizing and dissociating H₂ molecules, where interference between rotational, vibrational and electronic degrees of freedom leads to complex resonances that give a highly structured continuum with time scales spanning orders of magnitude. The dynamics of competing ionization and dissociation in molecules,[22] as well as the coherent control thereof,[23–25] has been of considerable interest for a long time. Just as in photochemistry,[26,27] there

are strong couplings between different degrees of freedom leading to radiationless transitions. The strongly nonadiabatic dynamics can be modeled with spectroscopic accuracy by multichannel quantum defect theory and we use a time-dependent formulation thereof[28] to map the dynamics induced by a range of phase-modulated optical pulses. We demonstrate that optical phase matched to the internal phase of the molecule can change the relative timing of ionization and dissociation and the width of the continuum fluxes. This has obvious implications for pump-dump style experiments; following the phase-shaped pump pulse with a conveniently timed dump pulse would give different final yields of products. For a single optical pulse, as studied here, the integrated final product yields are determined by the pulse envelope and are independent of the phase[29] in the weak-field domain.

II. THE SPECTRAL REGION OF H₂

Dipole excitation of ground state H₂ molecules to the region just above the ionization threshold H₂⁺ ($v^+=0, N^+=0$) is dominated by $p(l=1)$ partial waves and corresponds to the singlet ungerade spectrum of H₂ ($J=1$, negative total parity). A Rydberg series with effective principal quantum number $\nu \geq 26$ appears above the ionization threshold and converges toward the rotationally excited ($v^+=0, N^+=2$) limit, 174.2 cm⁻¹ above threshold. In addition, two vibrationally excited levels with lower electronic principal quantum number are present in the range, $7p\pi, v=1$ and $5p\pi, v=2$. All of these levels are embedded in the ionization continuum corresponding to H₂⁺ $X\,^2\Sigma_g^+$ ($v^+=0, N^+=0$) + $e^-(l=1)$ and the dissociation continua associated with the $B'\,^1\Sigma_u^+$ and $C\,^1\Pi_u$ electronic states converging to the H($1s$)+H($n=2$) dissociation threshold.

Figure 1 presents the photoionization and photodissociation dipole transition moments $D_{ks}^-(E)$ calculated for this range, with both the amplitude $|D_{ks}^-(E)|$ and the phase $\arg(D_{ks}^-(E))$ plotted. Only the dominant $B'\,^1\Sigma_u^+$ dissociation channel is included. Throughout this paper ionization refers to the H₂⁺ ($v^+=0, N^+=0$) channel and dissociation to the $B'\,^1\Sigma_u^+$ channel. In Fig. 1 it can be seen that the preionized

a)Present address: Laboratoire Aimé Cotton du CNRS, Université de Paris-Sud, 91405, Orsay, France.

b)Electronic mail: h.h.fielding@ucl.ac.uk.

c)Also at: Department of Physics and Astronomy, University College London, Gower Street, London WC1E 6BT, United Kingdom.
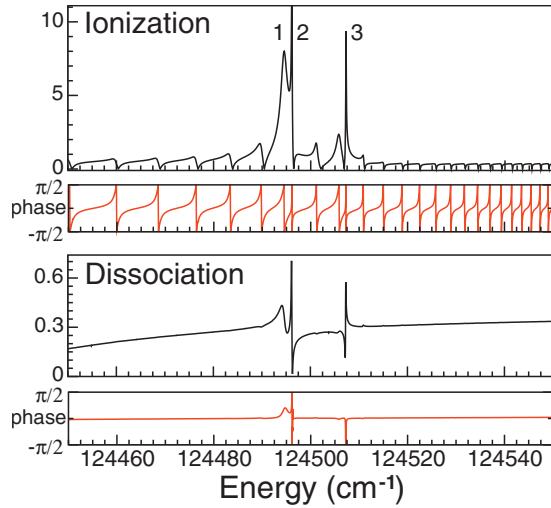
d)Electronic mail: christian.jungen@lac.u-psud.fr.

FIG. 1. Partial dipole transition moments $|D_{ks}^-(E)|$ (arb. units) for photoionization $H_2^+(v^+=0, N^+=0) + e^-(l=1)$ (top panel) and photodissociation $B'^1\Sigma_u^+$ $H+H(n=2)$ (bottom panel). The corresponding phase $\arg(D_{ks}^-(E))$ is shown below each panel. Details on the three resonances, referred to as 1, 2, and 3, are given in Table I.

$(v^+=0, N^+=2)$ Rydberg series consists of broad preionized peaks visible only in the photoionization spectrum, except for the $\nu=34$ peak near 124 494 cm^{-1} (label 1) which appears in both photoionization and photodissociation. The interlopers $7p\pi, \nu=1$ and $5p\pi, \nu=2$ (labels 2 and 3) are much sharper and appear both in photoionization and photodissociation.

Table I gives the calculated resonance positions for the two interloper resonances and the $\nu=34$, $(v^+=0, N^+=2)$ peak labeled in the spectrum in Fig. 1, along with the best available experimental positions and the widths estimated from the calculated spectrum. The table also gives the characteristic time scales associated with the three main components of each complex resonance. First, the lifetimes, $\tau_i = 1/\Delta E_i$, corresponding to the approximate width ΔE_i of each resonance i, second the beats, $\tau_{ij} = 2\pi/\Delta E_{ij}$, associated with the quantum beating between the coherently excited resonances i and j separated by energy ΔE_{ij}, and finally the Kepler times, $T_{cl} = 2\pi\nu^3$ au, i.e., the classical period of the Rydberg electron in channels $(v^+=0, N^+=2)$, $(v^+=2, N^+=2)$ and $(v^+=1, N^+=2)$, respectively. Note how these different intrinsic time scales of the system span almost two orders of magnitude.

III. THEORY

The energy domain representation of the rotating wave component of an optical pulse is

$$\epsilon(E) = \widetilde{\epsilon}_0 e^{-\alpha^2(E-E_0)^2} e^{\iota\Phi(E)}, \tag{1}$$

where $\widetilde{\epsilon}_0$ is the energy domain amplitude and the factor $\alpha = \sqrt{2\ln 2}/\tau_\omega$ is defined in terms of the full width at half maximum (FWHM) spectral width τ_ω, with the corresponding pulse duration $\tau_t = 4\ln 2/\tau_\omega$. Finally, $\Phi(E)$ is the phase profile, or spectral phase, of the pulse. A nonlinear spectral phase will lead to a chirp in the time domain. The focus of the present work is the effect on molecular dynamics of complicated spectral phases, which at least in principle could be generated[1] and characterized[39] experimentally. The complicated nature of the spectral phase makes the carrier envelope phase, shown to be important in the strong-field, few-cycle regime,[30] a less useful characteristic here. We also point out that given the large number of optical cycles under the pulse envelope, the zero area theorem[31] is generally fulfilled.

According to first order perturbation theory, the continuum wave packet at times beyond the duration of the pulse is

$$|\Psi_k^-(r,t)\rangle = 2\pi\iota \int dE D_{ks}^-(E)\epsilon(E)e^{-\iota Et/\hbar}|\Psi_k^-(r,E)\rangle, \tag{2}$$

for the target state k and dipole transition moment $D_{ks}^-(E)$. The product $D_{ks}^- \times \epsilon$ in Eq. (2) has dimension energy$^{-1/2}$; it determines the amplitude and phase of the contribution of each energy E to the wave packet depending on the transition moment and pulse characteristics. The wave functions $|\Psi_k^-(r,E)\rangle$ [and consequently the dipole transition moments $D_{ks}^-(E)$] are constructed according to outgoing boundary conditions, such that asymptotically each wave function k only carries amplitude in channel k for times $t\to\infty$. The probability density of the wave packet is given by the square modulus, i.e., $|\langle i|\Psi_k^-(r,t)\rangle|^2$ in each channel i, while the radial probability flux, j_i, associated with channel i is

$$j_i = \frac{\hbar}{m_\mu}\mathrm{Im}\left[\langle\Psi_k^-(r,t)|i\rangle\frac{\partial}{\partial r}\langle i|\Psi_k^-(r,t)\rangle\right], \tag{3}$$

where m_μ is the reduced mass. In the present paper, we focus on the probability fluxes in the open ionization and dissociation channels.

Further details on the theory can be found in Ref. 28. For the purpose of the present paper, it is useful to point out the following:[33,34]

- The treatment is unified in the sense that the electronic (ionization) and nuclear (vibrational) continua, and associated wave packet motions, are treated within a single framework.

TABLE I. Complex resonances in singlet ungerade H_2.

Resonance	Approximate[a] description	Calc. energy (cm^{-1})	Obs.[b] energy (cm^{-1})	Calc. width (cm^{-1})	Lifetime (ps)	Beat time (ps)	Kepler time (ps)
1	$34p, v^+=0$	124 494.5	124 495.5[c]	1.4	3.8	$\tau_{12}=21$	6.3
2	$5p\pi, \nu=2$	124 496.1	124 495.5[c]	0.15	35	$\tau_{23}=3.0$	0.02
3	$7p\pi, \nu=1$	124 507.3	124 507.2	0.09	59	$\tau_{13}=2.6$	0.05

[a]Hund's case b: $\nu l\lambda$, ν'. Hund's case d: $\nu l N^+$, v^+.
[b]Reference 32.
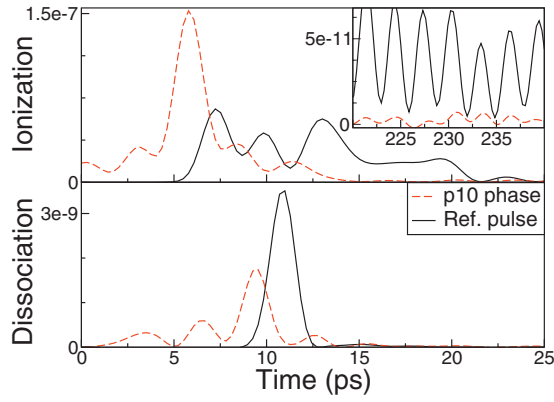[c]Blended pair of spectral lines.

FIG. 2. Ionization and dissociation flux calculated for phase profile p10 and the zero-phase reference pulse. The ionization flux in channel $H_2^+(v^+=0,N^+=0)+e^-(l=1)$ is calculated at $r_f=9000$ a.u. (top panel), and the dissociation flux in channel $B'\ {}^1\Sigma_u^+$ $H+H(n=2)$ at $R_f=3536$ a.u. (bottom panel). With phase profile p10 the bulk of the flux appears earlier, and the asymptotic flux is much smaller at long times (insert in top panel). The dissociation flux is also advanced by phase profile p10, but to a much lesser extent. While phase profile p10 focuses the ionization flux, it disperses the dissociation flux.

- It is based entirely on available *ab initio* potential energy curves of H_2 and the ion core, and thus constitutes a calculation from first principles.

- The calculation concerns a highly perturbed portion of the absorption spectrum of the hydrogen molecule and we have good agreement of the time-independent cross-section calculation with the available spectroscopic evidence[32,35,36] (see Table I).

The final product yields in each channel are proportional to the square amplitude of the partial cross sections and the optical pulse envelope, $|D_{ks}^-(E)|^2|\epsilon(E)|^2$, and hence independent of phase. On the other hand, the dynamics is highly sensitive to the optical phase, as demonstrated below.

Finally, a remark concerning units is in order. Natural units for electron scattering are used throughout, unless otherwise specified. This renders the flux in Eq. (3) and in Figs. 2–5 dimensionless.[28]

IV. CALCULATION

The dynamics of the H_2 molecule, including ionization and dissociation, is calculated for excitation by a range of optical pulses, all with the same Gaussian pulse envelope (FWHM width $\tau_E=9.0$ cm^{-1}, duration $\tau_T=1.6$ ps) centered between resonances 2 and 3 at $E_0=124\,500$ cm^{-1}, but different phase profiles $\Phi(E)$ [see Eq. (1)]. The phase profiles included in the calculations are listed in Table II and described below. Note that the integrated ratio of ionization (Y_{ion}) and dissociation (Y_{diss}) is $Y_{\text{ion}}/Y_{\text{diss}}=65$, independent of the phase profile used. The high ratio reflects that ionization is the dominant process in this region of the spectrum.

We explore the effects of an optical phase opposite to the phase of the dipole transition moment $D_{ks}^-(E)$, such that $\arg(D_{ks}^-\times\epsilon)=\arg(D_{ks}^-(E))+\Phi(E)=0$ and hence
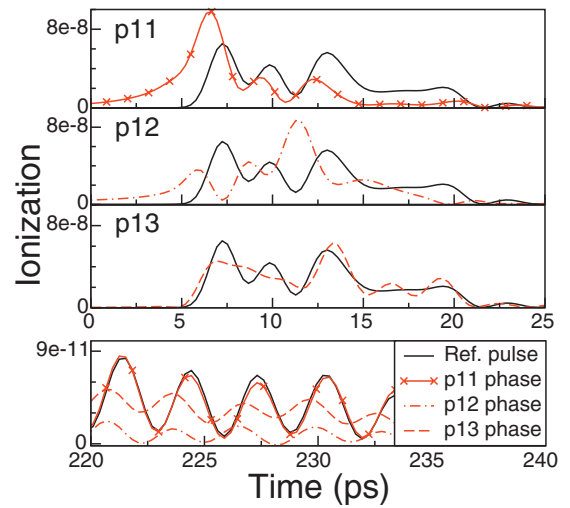

FIG. 3. Ionization flux in channel $H_2^+(v^+=0,N^+=0)+e^-(l=1)$ calculated at $r_f=9000$ a.u. The top three panels show the flux for the phase profiles p11 (top), p12 (middle) and p13 (bottom), with the ionization flux from the zero-phase reference pulse included for comparison in each panel. The effect of each phase profile on the flux is inversely proportional to the lifetime of corresponding resonance. Correspondingly, the greatest effect occurs for phase p11, which affects the most short-lived resonance 1. The fourth, bottom, panel shows the fluxes at asymptotic times. Here, the change in flux is proportional to the lifetime of each resonance, with the strongest effect for the most long-lived resonance 3.

$$\Phi(E) = -\arg(D_{ks}^-(E)), \qquad (4)$$

which we refer to as "counterphase." Since $\langle i|\Psi_k^-(r,E)\rangle \propto \exp(+\iota k_i(r,E))+\exp(-\iota k_i(r,E))\mathbf{S}_{ik}^-(E)$, where $\mathbf{S}^-$ is the asymptotic Hermitian scattering matrix, all phase-shifts in the outgoing wave packet originate from the term $(D_{ks}^-\times\epsilon)$ in Eq. (2). The phases $\arg(D_{ks}^-(E))$ are shown in Fig. 1 for both ionization and dissociation. First, we examine the counterphase for photoionization. The phase profile p10 corresponds to the counterphase for photoionization across the whole spectrum, i.e., at all energies. The counterphases p11, p12, and p13 only retain the photoionization counterphase at each of the three resonances, corresponding to the energy intervals [124 490.690, 124 495.771] (p11), [124 495.641, 124 496.476] (p12), and [124 506.895, 124 508.421] cm^{-1}

FIG. 4. Ionization flux in channel $H_2^+(v^+=0,N^+=0)+e^-(l=1)$ (top panel) and dissociation flux in channel $B'\ {}^1\Sigma_u^+$ $H+H(n=2)$ (bottom panel) calculated at $r_f=9000$ a.u. and $R_f=3536$ a.u. for the cosine phase profile. The zero-phase flux is included for reference. The optical pulse train, which results from the cosine phase, is clearly visible in the dissociation flux, but not in the ionization flux.
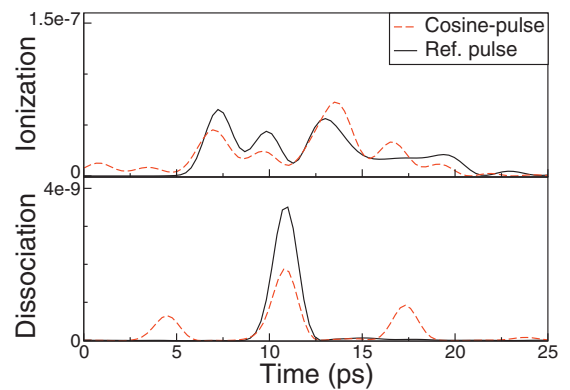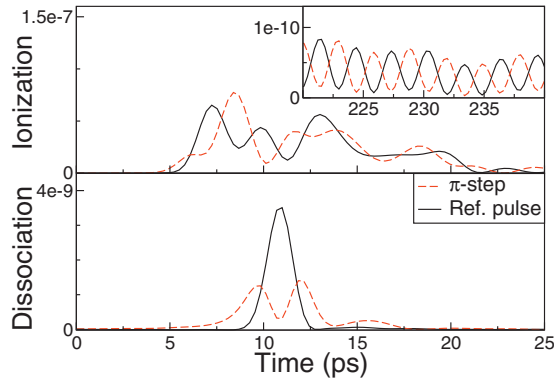
FIG. 5. Ionization flux in channel $H_2^+(v^+=0,N^+=0)+e^-(l=1)$ (top panel) and dissociation flux in channel $B'\ ^1\Sigma_u^+\ H+H(n=2)$ (bottom panel) calculated at $r_f=9000$ a.u. and $R_f=3536$ a.u. for the π phase step. The insert shows the ionization flux at long times and the zero-phase flux is included for reference. The beat pattern in the ionization flux, corresponding to beating between resonances 1–2 and 3 (short times) and resonances 2 and 3 (long times) is shifted by π. The dissociation flux has a double-peaked structure consistent with the double-peaked optical pulse resulting from the π phase step.

(p13). Outside these intervals, the phase profiles p11, p12 and p13 are flat. We also investigate the counterphase for photodissociation, p20, defined at all energies. In addition, we investigate the effect of a π phase step

$$\Phi(E) = \pi\mathbf{H}(E - E'), \tag{5}$$

where $\mathbf{H}$ is the Heaviside step-function and the energy $E' = 124\,502.08$ cm^{-1} corresponds to a minimum in the photo-ionization dipole transition moment between the resonances 2 and 3. This phase generates a double-peaked optical pulse in the time domain.[12,37] As a final example, we calculate the dynamics resulting from a cosine phase

$$\Phi(E) = \cos\beta(E - E_0), \tag{6}$$

for $\beta=1.2$ and with energy E in units of cm^{-1}. This value of β gives a temporal sequence of three optical pulses spaced by 6.4 ps.[12] Throughout, comparison is made with a reference pulse with constant phase, $\Phi(E)\equiv 0$.

TABLE II. Energy (frequency) dependent optical phases $\Phi(E)$ used in the calculations. For further details see Sec. IV and Eq. (1). In the text, the phase functions are referred to by the names given in this table.

Optical phase $\Phi(E)$	Description
p10	$\Phi(E)=-\arg(D_{ks}^-(E))$ (ionization)[a]
p11	Phase p10 at resonance 1 only, flat elsewhere
p12	Phase p10 at resonance 2 only, flat elsewhere
p13	Phase p10 at resonance 3 only, flat elsewhere
p20	$\Phi(E)=-\arg(D_{ks}^-(E))$ (dissociation)[a]
π-step	$\Phi(E)=\pi\mathbf{H}(E-E')$
Cosine	$\Phi(E)=\cos\beta(E-E_0)$
Reference	$\Phi(E)\equiv 0$

[a]See molecular phases in Fig. 1.

V. RESULTS AND DISCUSSION

A. Reference pulse dynamics

We will now discuss the ionization and dissociation probability fluxes calculated according to Eq. (3) and induced by the reference (zero-phase) optical pulse, which are shown in Fig. 2. The top panel in Fig. 2 shows the outgoing electron flux as a function of time in the open ionization channel $(v^+=0,N^+=0)$ calculated at radial distance $r_f=9000$ a.u. The ionization limit for this channel is 83 cm^{-1} below the center of the optical pulse, $E_0=124\,500$ cm^{-1}, which gives an asymptotic classical velocity of $v_i=1137$ $a_0$ps^{-1} for the ionized electron. The first peak, corresponding to direct ionization, arrives at 7.2 ps. This is earlier than the 7.9 ps (r_f/v_i) expected from the asymptotic velocity, but consistent with the higher electron velocity in the inner, attractive, region of the Coulomb potential.

The first three peaks are followed by a plateau region, which on close inspection contains two more peaks obscured by the background flux. These five peaks, spaced by approximately 3 ps, show an alternating pattern of intensity, due to the combination of Kepler motion in the closed $(v^+=0,N^+=2)$ Rydberg channel and the beating times τ_{13} and τ_{23} (see Sec. II). This alternating pattern dies out after the population in the closed Rydberg channel has vanished. At longer times, only the beating between the two long-lived resonances 2 and 3 persists (see insert in top panel Fig. 2). The peaks are now seen with intervals of 3.0 ps corresponding to τ_{23}.

The bottom panel in Fig. 2 shows the dissociation flux of neutral $H(1s)+H(n=2)$ atoms calculated at internuclear distance $R_f=3536$ a.u. The dissociation limit is 6124 cm^{-1} below the center of the pulse, giving a classical dissociation velocity of $v_d=324$ a_0 ps^{-1}. The first dissociation peak arrives 10.9 ps after the pulse, in very close agreement with what is expected on classical grounds (R_f/v_d). This is not surprising, since dissociation proceeds on an essentially flat potential. The flux is strongly dominated by the initial peak, reflecting the relatively featureless dissociation dipole transition moment in Fig. 1.

B. Dynamics with optical counterphases

In Fig. 2 we compare the ionization and dissociation probability fluxes calculated for the autoionization counterphase p10 with those for the reference pulse. Both the ionization and the dissociation flux are shifted to earlier times, but the ionization flux to a greater degree. Half of the total yield appears by $T_i^{1/2}=13.7$ ps (ionization flux) and $T_d^{1/2}=10.9$ ps (dissociation flux) with the zero-phase reference pulse. For the shaped phase p10, corresponding times are $T_i^{1/2}=6.1$ ps and $T_d^{1/2}=9.2$ ps. Hence, ionization is shifted by 7.6 ps, while dissociation is shifted by 1.7 ps only. The faster time scale for ionization with the shaped pulse is also confirmed by the reduced ionization flux at long times (see insert in top panel). Since the phase p10 cancels the phase of the photoionization dipole transition moment D_{ks}^-, it reduces the initial dispersion in the dynamics and gives flux, which is focused (localized) in one dominant peak. This is similar to optics, where the shortest-duration (bandwidth limited) pulses are realized when the phase dispersion is minimal,

i.e., when the phase is flat.[38,39] Conversely, the dissociation flux, which has a relatively flat phase $\arg(D_{ks}^-)$ to begin with, is dispersed by adding the autoionization counterphase.

The results in Fig. 2 can be examined by trying to disentangle the effect of the rather complicated phase p10. We do this by isolating different sections of the phase profile, which correspond to the different resonances, labeled 1–3 in Table I. These phase profiles are p11, p12, and p13, respectively, and the calculated ionization fluxes are shown in Fig. 3. The top three panels show the flux at early times, where the effect of each phase profile stands in proportion to the amount of early flux provided by the corresponding resonance. Hence, the effect of phase p11, which manipulates resonance 1, the most short-lived and broadest resonance, is greatest at early times. Correspondingly, the phase profiles corresponding to the two more long-lived resonances, p12 and p13, have a modest effect at short times. In particular, profile p13 associated with the most long-lived resonance 3 has very little effect.

We expect the opposite situation at large times, with the flux modified most strongly by the phase profiles associated with more long-lived resonances. The fluxes at long times are shown in the bottom panel in Fig. 3 (only the ionization flux is included, since the dissociation flux at these times is negligible). As expected, the phase profile p11, corresponding to the short-lived resonance 1, is almost identical to the reference pulse, while phase profiles p12 and p13 have a much greater effect, with the effect being the strongest for the most long-lived resonance 3. Note also that the fluxes for pulses p12 and p13 are somewhat shifted in phase.

Can a similar effect be achieved for the dissociation flux? The calculation with the photodissociation counterphase p20 (not shown in the figures) leads to a narrower and marginally ($\ll 1$ ps) earlier peak in the dissociation flux. The small effect is consistent with the almost flat photodissociation dipole transition moment in Fig. 1; the dissociation flux with the reference pulse is already focused in one peak, see, e.g., Fig. 2. Similarly, the flat photodissociation counterphase has only a small effect on the photoionization flux.

C. Dynamics with cosine phase and π phase step

Finally we investigate the effect of two common phase-profiles, a cosine phase and a π phase step. The cosine phase profile generates a pulse train with three pulses. These three pulses are nicely reproduced in the dissociation flux, shown in Fig. 4 (bottom panel). Conversely, the rapidly changing phase in the photoionization dipole transition moment scrambles the optical phase and renders the ionization flux quite different from the optical excitation pulse (Fig. 4, top panel).

For a π-step we see in Fig. 5 how the beats in the ionization flux (top panel) are shifted out of phase compared with the zero-phase reference pulse. At short times the beating between resonances 1–2 and resonance 3 is inverted. This π shift in the flux is even more visible at long times (insert) when only the beating between resonances 2 and 3 survives. Just as in the case of the cosine phase, the temporal structure of the optical pulse remains visible in the dissocia-

tion flux (bottom panel); here a double-peak generated by the π-step.[37] As in the case of a cosine phase previously, this is because the almost flat photodissociation phase preserves the optical phase.

VI. CONCLUSIONS

We have demonstrated the influence of optical phase on molecular dynamics in highly excited, ionizing and dissociating, H_2 molecules. Most strikingly, we are able to change the relative timing of ionization and dissociation by an appropriate choice of phase. This is possible thanks to the large difference between the dipole transition moments for the two processes.

In a broader context, our results emphasize the effect of the optical phases on the dynamics of the molecular wave packet. The phase of the wave packet originates both from the molecule [in our calculations through $\arg(D_{ks}^-(E))$] and from the optical pulse. In every case examined in this paper, the same states are excited with the same final amplitudes, giving identical product yields, but the differences in optical phase lead to dramatically different evolution of the ionizing and dissociating wave packets.

An interesting example of the interplay between molecular and optical phase is provided by the difference between the fluxes resulting from the π phase step optical pulse. The distinct temporal structure of the optical pulse is preserved in the dissociation flux, which is almost a flat continuum, while the ionization flux bears no such resemblance because the rapidly varying phase in the ionization continuum completely scrambles the temporal structure of the optical pulse. The strong effect of the molecular phase suggests that further investigation of dynamics for complex superpositions of resonances should be interesting.[40,41]

Our results underscore previous and well-established warnings to be careful about inferring dynamics from measurements with pulses with substantially distorted phase.[39] Most importantly, these results indicate how calculated molecular phases could guide the design of phase patterns to manipulate the dynamics in complex molecular systems.

[1] A. M. Weiner, Rev. Sci. Instrum. **71**, 1929 (2000).
[2] R. S. Judson and H. Rabitz, Phys. Rev. Lett. **68**, 1500 (1992).
[3] A. Assion, T. Baumert, M. Bergt, T. Brixner, B. Kiefer, V. Seyfried, M. Strehle, and G. Gerber, Science **282**, 919 (1998).
[4] M. Dantus and V. V. Lozovoy, Chem. Rev. (Washington, D.C.) **104**, 1813 (2004).
[5] K. Ohmori, Annu. Rev. Phys. Chem. **60**, 487 (2009).
[6] M. W. Noel and J. C. R. Stroud, Opt. Express **1**, 176 (1997).
[7] F. Texier and F. Robicheaux, Phys. Rev. A **61**, 043401 (2000).
[8] R. S. Minns, R. Patel, J. R. R. Verlet, and H. H. Fielding, Phys. Rev. Lett. **91**, 243601 (2003).
[9] J. R. R. Verlet, V. Stavros, R. S. Minns, and H. H. Fielding, Phys. Rev. Lett. **89**, 263004 (2002).

[10] J. R. R. Verlet, V. G. Stavros, R. S. Minns, and H. H. Fielding, J. Phys. B **36**, 3683 (2003).

[11] R. E. Carley, E. D. Boleat, R. S. Minns, R. Patel, and H. H. Fielding, J. Phys. B **38**, 1907 (2005).

[12] M. Renard, R. Chaux, B. Lavorel, and O. Faucher, Opt. Express **12**, 473 (2004).

[13] B. Kohler, V. V. Yakovlev, J. Che, J. L. Krause, M. Messina, K. R. Krause, N. Schwentner, R. M. Whitnell, and Y. Yan, Phys. Rev. Lett. **74**, 3360 (1995).

[14] C. J. Bardeen, J. Che, K. R. Wilson, V. V. Yakovlev, V. A. Apkarian, C. C. Martens, R. Zadoyan, B. Kohler, and M. Messina, J. Chem. Phys. **106**, 8486 (1997).

[15] J. C. Delagnes and M. A. Bouchene, J. Phys. B **35**, 1819 (2002).

[16] M. A. Bouchene, Phys. Rev. A **68**, 023401 (2003).

[17] A. Kirrander, Ch. Jungen, and H. H. Fielding, J. Phys. B **41**, 074022 (2008).

[18] J. A. Yeazell and J. C. R. Stroud, Phys. Rev. Lett. **60**, 1494 (1988).

[19] A. ten Wolde, L. D. Noordam, A. Lagendijk, and H. B. van Linden van den Heuvell, Phys. Rev. Lett. **61**, 2099 (1988).

[20] J. L. Krause, K. J. Schafer, M. Ben-Nun, and K. R. Wilson, Phys. Rev. Lett. **79**, 4978 (1997).

[21] T. C. Weinacht, J. Ahn, and P. H. Bucksbaum, Nature (London) **397**, 233 (1999).

[22] T. Baumert, B. Bühler, R. Thalweiser, and G. Gerber, Phys. Rev. Lett. **64**, 733 (1990).

[23] T. Baumert, M. Grosser, R. Thalweiser, and G. Gerber, Phys. Rev. Lett. **67**, 3753 (1991).

[24] L. Zhu, V. Kleiman, X. Li, S. P. Lu, K. Trentelman, and R. J. Gordon, Science **270**, 77 (1995).

[25] L. Zhu, K. Suto, J. A. Fiss, R. Wada, T. Seideman, and R. J. Gordon, Phys. Rev. Lett. **79**, 4108 (1997).

[26] A. Tramer, Ch. Jungen, and F. Lahmani, *Energy Dissipation in Molecular Systems*, 1st ed. (Springer, New York, 2005).

[27] A. H. Zewail, F. C. de Schryver, S. D. Feyter, and G. Schweitzer, *Femtochemistry: With the Nobel lecture of A. Zewail*, 1st ed. (Wiley-VCH GmbH, Weinheim, Germany, 2001).

[28] A. Kirrander, H. H. Fielding, and Ch. Jungen, J. Chem. Phys. **127**, 164301 (2007).

[29] M. Shapiro and P. Brumer, *Principles of the Quantum Control of Molecular Processes*, 1st ed. (Wiley, New York, 2003).

[30] A. D. Bandrauk, S. Chelkowski, and N. H. Shon, Phys. Rev. Lett. **89**, 283903 (2002).

[31] S. Chelkowski and A. D. Bandrauk, Phys. Rev. A **71**, 053815 (2005).

[32] G. Herzberg and Ch. Jungen, J. Mol. Spectrosc. **41**, 425 (1972).

[33] Ch. Jungen and S. C. Ross, Phys. Rev. A **55**, R2503 (1997).

[34] F. Texier, Ch. Jungen, and S. C. Ross, Faraday Discuss. Chem. Soc. **115**, 71 (2000).

[35] P. M. Dehmer and W. A. Chupka, J. Chem. Phys. **65**, 2243 (1976).

[36] M. Glass-Maujean, J. Breton, and P. M. Guyon, Z. Phys. D: At., Mol. Clusters **6**, 189 (1987).

[37] A. Kirrander and H. H. Fielding, J. Phys. B **40**, 897 (2007).

[38] L. Cohen, Proc. IEEE **77**, 941 (1989).

[39] R. Trebino, *Frequency-Resolved Optical Gating: The Measurement of Ultrashort Laser Pulses*, 1st ed. (Springer, New York, 2002).

[40] M. Shapiro, J. Phys. Chem. A **102**, 9570 (1998).

[41] P. S. Christopher, M. Shapiro, and P. Brumer, J. Chem. Phys. **125**, 124310 (2006).